ELSEVIER

Journal of Applied Geophysics 45 (2000) 83–96

JOURNAL OF APPLIED GEOPHYSICS

www.elsevier.nl/locate/jappgeo

Numerical analysis of 2.5-D true-amplitude diffraction stack migration

J.C.R. Cruz *, J. Urban, G. Garabito

Received 1 January 2000; accepted 19 May 2000

Abstract

By considering arbitrary source–receiver configurations, compressional primary reflections can be imaged into time or depth-migrated seismic sections so that the migrated wavefield amplitudes are a measure of angle-dependent reflection coefficients. Several migration algorithms were proposed in the recent past based on the Born or Kirchhoff approach. All of them are given in form of a weighted diffraction-stack integral operator that is applied to the input seismic data. The result is a migrated seismic section where at each reflection point the source wavelet is reconstructed with an amplitude proportional to the reflection coefficient at that point. Based on the Kirchhoff approach, we derive the weight function and the diffraction stack integral operator for a two and one-half (2.5-D) seismic model and apply it to a set of synthetic seismic data in noisy environment. The result shows the accuracy and stability of the 2.5-D migration method as a tool for obtaining important information about the reflectivity properties of the earth's subsurface, which is of great interest for amplitude vs. offset (angle) analysis. We also present a new application of the Double Diffraction Stack (DDS) inversion method to determine three important parameters along the normal ray path, i.e., the angle and point of emergence at the earth surface, and also the radius of curvature of the hypothetical Normal Incidence Point (NIP) wave.

Keywords: Imaging; Ray; Migration; Inversion

1. Introduction

In the recent years, we have seen an increasing interest in true amplitude migration methods. A major part of these works dealt with this topic either based on the Born approximation as given by Bleistein (1987) and Bleistein et al. (1987), or on the ray theoretical wavefield approximation as given by Hubral et al. (1991) and Schleicher et al. (1993).

This paper follows the latter alternative of working the migration problem by using the ray theoretical approximation. We consider a geophysical situation where the propagation velocity of a point-source wave does not vary along one of the three-dimensional (3-D) Cartesian coordinate axes, the so-called two and one-half (2.5-D) model.

* Corresponding author. Centro de Geosciencas, Universidade Federal do Para, CP 1611, AV. Bernardo Sayao, 01, 66017-900 Belem-Para, Brazil. Fax: +55-91-211-1693.

E-mail addresses: jcarlos@ufpa.br (J.C.R. Cruz), urban@ufpa.br (J. Urban), german@ufpa.br (G. Garabito).

0926-9851/00/$ - see front matter
PII: S0926-9851(00)00020-3

Starting from the 3-D weighted modified diffraction stack operator as presented by Schleicher et al. (1993), we derive the appropriate method to perform a 2.5-D true-amplitude seismic migration. We find the weight function to be applied to the amplitude of the 2.5-D seismic data.

In summary, the paper presents a theoretical development by which we derive an expression for the 2.5-D weight that is a function of ray parameters. We show examples of application of the true-amplitude depth migration algorithm to 2.5-D synthetic seismic data in noisy environment in order to make the numerical analysis more realistic and to verify the stability and accuracy of the algorithm. In the final part, based on the theoretical development given by Bleistein (1987) and Tygel et al. (1993), we apply the Double Diffraction Stack (DDS) inversion method to determine normal ray parameters, which are the keys for a more general interval velocity inversion problem.

2. Review of 2.5-D ray theory

2.1. The seismic model

We use the general Cartesian coordinate system being the position vector $\boldsymbol{x} = (x, y, z)$. One of the main concerns of this paper is to apply the ray field properties to the 2.5-D seismic model in order to study the true-amplitude seismic migration method. We think of the earth as a system of isotropic layers, where each layer is constituted by a velocity field $v = v(\boldsymbol{x})$, whose first derivative with respect to the second component y vanishes in all space. Each layer has smooth surfaces as upper and lower bounds. The upper bound surface Σ_0 is the earth surface. The curvature of each surface is zero along the second component y-axis, i.e., the seismic model has a cylindrical symmetry on the y direction (Fig. 1). The intersection between the plane of symmetry $y = 0$ and the earth surface Σ_0 defines the seismic line. In the 2.5-D seismic model, the wave velocity does not vary along the y direction, while the point-source seismic wave causes 3-D propagation.

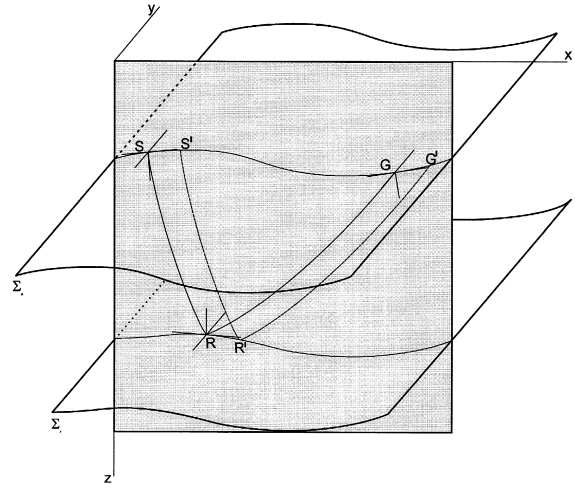

Fig. 1. 2.5-D seismic model. The in-plane central and paraxial rays start at the earth surface. After reflecting at the reflector, they reach the receiver positions.

At our seismic experiment carried out on Σ_0, we consider only P–P primary reflections to be registered at the source–receiver pairs (S, G). We assume reproducible point sources with unit strength and receivers with identical characteristics. Their position vectors are denoted by:

$$\mathbf{x}_s = \mathbf{x}_s(\boldsymbol{\xi}) \text{ and } \mathbf{x}_g = \mathbf{x}_g(\boldsymbol{\xi}), \tag{1}$$

where $\boldsymbol{\xi} = (\xi_1, \xi_2)$ is a vector of parameters on Σ_0.

The high frequency primary reflection wavefield trajectory is then described by a ray that starts at the source point S on Σ_0, reaches the reflector Σ_r at the reflection point R, defined by a vector $\boldsymbol{x}_r = \boldsymbol{x}_r(\boldsymbol{\eta})$, $\boldsymbol{\eta} = (\eta_1, \eta_2)$ being a vector of parameters within Σ_r, and returns to the earth surface at G, the ray path SRG. By considering the 2.5-D case, the ray path SRG is assumed to be totally contained in the plane $y = 0$.

We introduce three local Cartesian coordinate systems with the first two having their origins at

the points S and G with components (x_{1s}, x_{2s}, x_{3s}) and (x_{1g}, x_{2g}, x_{3g}), respectively. The third coordinate system has its origin at the point R with components (x_{1r}, x_{2r}, x_{3r}). The axes x_{1s} and x_{1g} are tangents to the seismic line, while x_{3s} and x_{3g} are downward normal to the Σ_o. The components (x_{1r}) and (x_{3r}) are defined in such a way that the former is tangent to the reflector Σ_r within the symmetry plane $y=0$, while the latter is upward normal to the reflector. The second components x_{2s}, x_{2g} and x_{2r} have the same direction as the y component in the general Cartesian coordinate system (Fig. 1).

2.2. Ray theory

The principal component primary reflection of the seismic wavefield generated by a compressional point source located at x_s and registered at x_g is expressed in the 3-D zero-order ray approximation given by Cervený (1987) as:

$$\mathbf{U}(\boldsymbol{\xi},t) = U_o W(t-\tau(\boldsymbol{\xi})). \tag{2}$$

The above cited principal component primary reflection describes the particle displacement into direction of the ray at the receiver point G. In Eq. (2), $W(t)$ represents the analytic point-source wavelet, i.e., this is a complex valued function whose imaginary part is the Hilbert transform of the real source wavelet, and the real part is the wavelet itself. At the receiver position x_g within the surface Σ_o, the seismic trace is the superposition of the principal component primary reflections.

The reflection traveltime function $\tau=\tau(\boldsymbol{x})$ satisfies the 3-D eikonal equation

$$\nabla\tau\cdot\nabla\tau = 1/v^2(\mathbf{x}), \tag{3}$$

Being $v=v(\boldsymbol{x})$ the P wave velocity. The amplitude factor U_o can be expressed by:

$$U_o = U_o v\nabla\tau, \tag{4}$$

where $U_o = U_o(\boldsymbol{x})$ is a scalar function that satisfies the 3-D transport equation, in constant density and varying velocity media, given by:

$$2(\nabla\tau\cdot\nabla U_o)v^2(\mathbf{x}) + v^2 U_o\nabla^2\tau + U_o(\nabla\tau\cdot\nabla v^2) = 0. \tag{5}$$

By considering only the 2.5-D wave propagation within the symmetry plane $y=0$, that is of interest, we assume $\xi_2=\eta_2=0$, $\xi_1=\xi$ and $\eta_1=\eta$, simplifying the notation, so that we have $\boldsymbol{x}_s=\boldsymbol{x}_s(\xi)$, $\boldsymbol{x}_g=\boldsymbol{x}_g(\xi)$ and $\boldsymbol{x}_r=\boldsymbol{x}_r(\eta)$.

Following Bleistein (1986), we introduce the fundamental *in-plane slowness vector*:

$$\mathbf{p} = (p,q) = \frac{\boldsymbol{t}}{v(\boldsymbol{x},z)} = \nabla\tau(\boldsymbol{x},z), \tag{6}$$

where the two-components unitary vector $\boldsymbol{t}$ is tangent to the in-plane ray trajectory. In Eq. (6), the components p and q are the so-called horizontal and vertical slowness, respectively, which are related to each other by the expression:

$$q = \pm\sqrt{\frac{1}{v^2}-p^2}\,. \tag{7}$$

By using the in-plane initial values of the slowness vector $\boldsymbol{p}_o=(p_o,q_o)$ given as:

$$p_o = \frac{\sin\beta_o}{v_o}, \quad q_o = \frac{\cos\beta_o}{v_o}, \tag{8}$$

where β_o and v_o are the start angle of the ray and the velocity at the source point S, respectively. The in-plane ray equations are alternatively described by:

$$\frac{\mathrm{d}\boldsymbol{x}}{\mathrm{d}\sigma} = p, \tag{9}$$

$$\frac{\mathrm{d}z}{\mathrm{d}\sigma} = q, \tag{10}$$

$$\frac{\mathrm{d}p}{\mathrm{d}\sigma} = \frac{\partial}{\partial x}\left[\frac{1}{v^2(\boldsymbol{x},z)}\right], \tag{11}$$

$$\frac{\mathrm{d}\tau}{\mathrm{d}\sigma} = \frac{1}{v^2(\boldsymbol{x},z)}, \tag{12}$$

where $\mathrm{d}\sigma = v(\boldsymbol{x},z)\mathrm{d}s$.

Applying the above in-plane ray equations, and considering the initial conditions (8), to the fundamental solution of the transport Eq. (5) as found in Cervený (1987), the amplitude factor of the in-plane reflected wavefield is computed by:

$$(U_o)_{2.5} = \frac{R_c \mathscr{A}}{\mathscr{L}_{2.5}} \approx \frac{R_c}{\mathscr{L}_{2.5}}. \quad (13)$$

In formula (13), R_c is the geometrical-optics reflection coefficient at the reflection point R as presented by Bleistein (1984). The factor $\mathscr{A}$ corresponds to the total lost energy due to the transmission across all interfaces along the whole ray. In general, we assume this factor to be negligible, i.e., the transmission loss to be very small, or to be corrected by other means. The amplitude factor $\mathscr{L}_{2.5}$ is called in-plane point-source divergence factor or *geometrical spreading*, whose expression will be given in the Section 2.3.

2.3. Paraxial ray approximation

The paraxial ray approximation is based on the a priori knowledge of a ray trajectory also known as the *central ray*, which in our example is the ray that starts at the source $S(\xi)$, reaches the reflector at the reflection point $R(\eta)$, and arrives at the receiver $G(\xi)$. Thus, a *paraxial ray* is any ray that starts in the vicinity of S, at the point $S'(\xi')$, reflects at the point $R'(\eta')$ nearby the point R, and reaches the receiver point $G'(\xi')$ in the vicinity of G (Fig. 1).

By applying the concept of paraxial rays, Cervený (1987) derived the paraxial eikonal equation having as solution the two-point paraxial reflection traveltime from point S' at $\boldsymbol{x}'_s = \boldsymbol{x}_s(\xi')$ to the point G' at $\boldsymbol{x}'_g = \boldsymbol{x}_g(\xi')$ in the vicinity of points S and G, respectively. An equivalent second-order approximation solution was found also by Ursin (1982) and Bortfeld (1989). In this paper, we use the formalism of Schleicher et al. (1993) tailored to the in-plane ray trajectory. The reflection traveltime is then given by:

$$\tau_R(s,g) = \tau_R(s=0, g=0) + p_G g - p_S s - sN_{SG} g + \frac{1}{2} N_S^G s^2 + \frac{1}{2} N_G^S g^2. \quad (14)$$

In Eq. (14), the function $\tau_R(s=0,\ g=0)$ denotes the traveltime along the central ray SG, while s and g are linear distances in the axes x_{1s} and x_{1g}, the so-called *paraxial distances*. These distances are obtained as follows: (1) At the source–receiver points S' and G', the vectors $\boldsymbol{x}'_s$ and $\boldsymbol{x}'_g$ are orthogonally projected onto the respective axis x_{1s} and x_{1g}; (2) the distances s and g are then defined as having origin at the source–receiver points S and G with end at the extremity of the projections of $\boldsymbol{x}'_s$ and $\boldsymbol{x}'_g$, respectively. On the other hand, the so-called *local horizontal slowness* p_S and p_G are obtained by two cascaded orthogonal projections of the initial and final in-plane slowness vectors at source–receiver points S' and G' onto the respective axes x_{1s} and x_{1g}.

The quantities N_S^G and N_G^S are second-derivatives of the traveltime function (14) with respect to the source and receiver coordinates evaluated at $s=0$ and $g=0$, respectively. The other quantity N_{SG} is the second-order mixed-derivative of the same traveltime function (14) evaluated at $s=g=0$.

In the next section, we will perform the 2.5-D true-amplitude migration by using a proper weighted modified diffraction stack. For that, we define for all points of parameters ξ on the earth surface, and each point M within a specified volume of the macro-velocity model, the diffraction in-plane traveltime curve:

$$\tau_D(\xi) = \tau(S,M) + \tau(M,G) = \tau_S + \tau_G. \quad (15)$$

Following Schleicher et al. (1993), we will refer to this curve as the *Huygens traveltime*. The traveltimes τ_S and τ_G denote, respectively, the traveltimes from the source point S to some

arbitrary point M within the model, and from M to the receiver point G.

For obtaining the Huygens paraxial traveltime at a reflection point within Σ_r in the vicinity of R at $\boldsymbol{x}_r = \boldsymbol{x}_r(\eta)$, $M = R'$ in Eq. (15), with position vector $\boldsymbol{x}'_r = \boldsymbol{x}_r(\eta')$, we consider two equations of type (14) for the paraxial traveltime from S' to R'

$$\tau(s,r) = \tau(s=0, r=0) - p_S s + p_r r - sN_{SR} r + \frac{1}{2} N_S^R s^2 + \frac{1}{2} N_R^S r^2, \tag{16}$$

and from R' to G'

$$\tau(r,g) = \tau(r=0, g=0) - p_r r + p_G g - rN_{RG} g + \frac{1}{2} N_R^G r^2 + \frac{1}{2} N_G^R g^2. \tag{17}$$

In both formulas (16) and (17), the quantity r is the linear distance between R and the extremity of the orthogonal projection of $\boldsymbol{x}'_r$ onto the axis x_{1r} tangent to the reflector at the point R. The local horizontal slowness p_r is built by two cascaded projections of the in-plane slowness vector at $\boldsymbol{x}_r$ onto the x_{1r} axis.

It is necessary to point out that in general, the earth surface is not a horizontal plane, instead, it can be even an arbitrary surface. In our case, we consider it as a smooth surface with cylindrical geometry with axis in direction of the y coordinate. Thus, s and g are paraxial distances evaluated within tangent planes to the earth surface at S and G, respectively. Moreover, $\boldsymbol{x}_s(\boldsymbol{x}'_s)$ and $\boldsymbol{x}_g(\boldsymbol{x}'_g)$ are position vectors of the points $S(S')$ and $G(G')$ in the general Cartesian coordinates. The same geometrical assumption is required for the reflector surface, by the way the paraxial distance r is evaluated within the tangent plane at the reflection point, while $\boldsymbol{x}_r$ $(\mathbf{x}'_r)$ are the position vectors of the points $R(R')$.

The quantities N_{SR} and N_{RG} are second-order mixed-derivatives, respectively of the traveltimes (16) and (17) calculated at $s = g = r = 0$, while N_S^R and N_R^S are the second-order derivatives of the traveltime function (16) with respect to s and r, respectively. The quantities N_R^G and N_G^R are the second-order derivatives of the traveltime function (17) with respect to r and g.

Following Bleistein (1986), Liner (1991), Stockwell (1995) and Hanitzsch (1997), the expression of the geometrical spreading factor, when tailored to the 2.5-D zero-order ray approximation of the seismic wavefield, is given by:

$$\mathscr{L}_{2.5} = \frac{\sqrt{\cos\alpha_S \cos\alpha_G}}{v_s} \frac{\sqrt{\sigma_S + \sigma_G}}{\sqrt{|\mathscr{N}|}} \times \exp\left[-i\frac{\pi}{2}\kappa\right]. \tag{18}$$

In the above formula (18), we have that α_S and α_G are the start and emergence angles of the central ray measured with respect to the normal at S and G on the earth surface, while v_s is the velocity at the source point S. The term $\mathscr{N}$ in the denominator is given by the ratio:

$$\mathscr{N} = \frac{N_{SR} N_{GR}}{N_R^S + N_R^G}. \tag{19}$$

Moreover, we have that σ_S and σ_G are two quantities related with each branch of the in-plane central ray SR and RG, and calculated by the expressions:

$$\sigma_S = \int_S^R v(\mathbf{x})\mathrm{d}s \text{ and } \sigma_G = \int_R^G v(\mathbf{x})\mathrm{d}s. \tag{20}$$

The exponential term in Eq. (18) represents the phase shift due to the caustics along each branch of the central ray. For obtaining this factor, it is necessary to use dynamic ray tracing.

From Eq. (18), the 2.5-D geometrical spreading $\mathscr{L}_{2.5}$ can be expressed then as function of the 2-D spreading $\mathscr{L}_2$, given by:

$$\mathscr{L}_{2.5} = \mathscr{L}_2 \mathscr{F}_{2.5}, \qquad \mathscr{F}_{2.5} = \sqrt{\sigma_S + \sigma_G}, \tag{21}$$

where $\mathscr{F}_{2.5}$ is called the out-of-plane factor. Essentially, the $\mathscr{L}_{2.5}$ depends only on parame-

ters of 2-D rays. The 2.5-D amplitude factor of the zero-order ray approximation is then rewritten as:

$$(U_o)_{2.5} = \frac{(U_o)_2}{\mathscr{F}_{2.5}}. \tag{22}$$

In the expression (22), we have that $(U_o)_2$ denotes the in-plane 2-D wavefield amplitude. An equivalent relationship between 2-D and 2.5-D amplitude factors can be found in Bleistein (1986). This means that if we know the 2-D amplitude factor, we need only to divide it by the out-of-plane factor $\mathscr{F}_{2.5}$ in order to obtain the 2.5-D amplitude.

3. 2.5-D ray migration theory

By following the zero-order ray approximation of the 2.5-D seismic wave, we have the true-amplitude defined as:

$$U_{\mathrm{TA}}(t) = \mathscr{L}_{2.5}(U_o)_{2.5}(\xi, t+\tau_R) = R_c W(t). \tag{23}$$

In order to build the appropriate true-amplitude migration operator, we start from the 3-D integral given by Schleicher et al. (1993):

$$V(M,t) = \frac{-1}{2\pi}\int\int_A \mathrm{d}\xi_1 \mathrm{d}\xi_2 w(\boldsymbol{\xi}, M)\dot{U} \left(\boldsymbol{\xi}, t+\tau_D(\boldsymbol{\xi}, M)\right), \tag{24}$$

where the symbol $(\cdot)$ means the first derivative with respect to time, and $w(\boldsymbol{\xi}, M)$ is the weight function used to stack.

By assuming the paraxial distances s and g to be linear functions of ξ, we can write:

$$s = \Gamma_S \xi \text{ and } g = \Gamma_G \xi, \tag{25}$$

where $\Gamma_S = (\partial s/\partial\xi)$ and $\Gamma_G = (\partial g/\partial\xi)$, which are calculated at $\xi = 0$. In the same way, we consider r a linear function of η so that:

$$r = \Gamma_r \eta, \text{ where } \Gamma_r = \frac{\partial r}{\partial \eta}. \tag{26}$$

As a consequence of the above relations (25) and (26), we can express the traveltime functions $\tau_R = \tau_R(\xi)$ and $\tau_D = \tau_D(\xi, R)$. Moreover, we can define the function $\tau_F(\xi, R) = \tau_D(\xi, R) - \tau_R(\xi)$.

By using the result obtained in the Appendix by Eq. (A8), we have the 2.5-D modified diffraction stack integral in frequency domain given by the stationary phase solution:

$$\hat{V}(R,\omega) \approx \frac{\sqrt{-i\omega}}{\sqrt{2\pi}}\int_A \mathrm{d}\xi\, w_{2.5}(\xi, R)\hat{U}_{2.5}(\xi,\omega) \times \exp\left[i\omega\tau_D(\xi, R)\right]. \tag{27}$$

Inserting the 2.5-D zero-order approximation (13) of the primary reflection into integral (27) we have:

$$\hat{V}(R,\omega) \approx \frac{\sqrt{-i\omega}}{\sqrt{2\pi}}\int_A \mathrm{d}\xi\, w_{2.5}(\xi, R)\frac{R_c}{\mathscr{L}_{2.5}}\hat{W}(\omega) \times \exp\left[i\omega\tau_F(\xi, R)\right]. \tag{28}$$

The above integral (28) is once again calculated approximately by the stationary phase method. At this time, we apply the stationary phase condition $(\partial\tau_F)/(\partial\xi)\,|_{\xi=\xi^*} = 0$. Thus, we have:

$$\hat{V}(R,\omega) \approx \hat{W}(\omega)\frac{w_{2.5}(\xi^*, R)}{\sqrt{|\tau_F''(\xi^*, R)|}} \times \frac{R_c}{\mathscr{L}_{2.5}} \times \exp\left[i\omega\tau_F(\xi^*, R) - \frac{i\pi}{4}\left(1 - \mathrm{Sgn}\left(\tau_F''(\xi^*, R)\right)\right)\right]. \tag{29}$$

Where $\tau_F''(\xi^*, R) = (\partial^2\tau_F(\xi, R)/\partial\xi^2)\,|_{\xi=\xi^*}$ is the second-order derivative of the Taylor expansion:

$$\tau_F(\xi, R) = \tau_F(\xi^*, R) + \frac{1}{2}\tau_F''(\xi^*, R)(\xi - \xi^*)^2. \tag{30}$$

After some algebraic manipulations involving the (14), (16) and (17), we can express the second-order derivative term by:

$$\tau_F'' = \frac{\left(\Gamma_S N_{SR} + \Gamma_G N_{GR}\right)^2}{\left(N_R^S + N_R^G\right)}. \qquad (31)$$

3.1. Weight function

The 2.5-D weight function at an arbitrary point M in the macro-velocity model through the high frequency approximation of the diffraction stack integral, for a critical point ξ^* within the migration apperture A. The weight function is then obtained so that the stack integral is asymptotically equal to the spectrum of the true-amplitude migrated source wavelet multiplied by a phase shift operator. In other words, the phase of the asymptotical result is shifted by a quantity equal to the difference between the in-plane reflection and diffraction traveltime curves at the stationary point. Thus, we have:

$$\hat{V}(M,\omega) \approx \begin{cases} R_c \hat{W}(\omega)\exp[i\omega\tau_F(\xi^*,M)] & : \quad \xi^* \in A \\ 0 & : \quad \xi^* \notin A \end{cases} \qquad (32)$$

By using the stationary phase approximation (29) and definition (32), the 2.5-D weight function is then obtained as:

$$w_{2.5}(\xi^*,M) = \mathscr{L}_{2.5}\sqrt{|\tau_F''(\xi^*,M)|} \times \exp\left[\frac{i\pi}{4}\left(1 - \mathrm{Sgn}\left(\tau_F''(\xi^*,M)\right)\right)\right]. \qquad (33)$$

After replacing the appropriate definition of $\mathscr{L}_{2.5}$ as given by Eq. (18) and including the evaluation of τ_F'' from the expression (31), we have the result:

$$w_{2.5}(\xi^*,M) = \mathscr{F}_{2.5}\frac{\sqrt{\cos\alpha_S \cos\alpha_G}}{v_s} \times \left(\frac{\Gamma_S N_{SM} + \Gamma_G N_{GM}}{\sqrt{N_{SM} N_{GM}}}\right) \times \exp\frac{-i\pi}{2}\left[\kappa_1 + \kappa_2\right]. \qquad (34)$$

Based on the 3-D weight function found in Tygel et al. (1996) by using the so-called Beylkin's determinant, Martins et al. (1997) derived a similar 2.5-D weight $w_J(\xi^*,M)$. This result is related with the 2.5-D weight function given in the present paper by:

$$w_{2.5}(\xi^*,M) = w_J(\xi^*,M)\exp\frac{-i\pi}{2}\left[\kappa_1 + \kappa_2\right]. \qquad (35)$$

The difference between both results can be explained by the assumption used in Beylkin

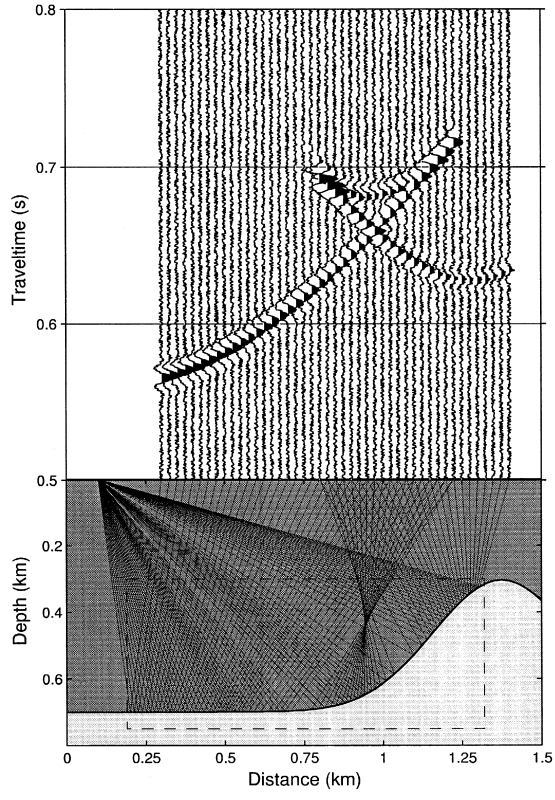

Fig. 2. Top: Synthetic seismic data used as input in the 2.5-D true-amplitude depth migration algorithm, with the signal-to-noise ratio equal to 1:0.1. Bottom: Seismic model used for the generating the synthetic data.

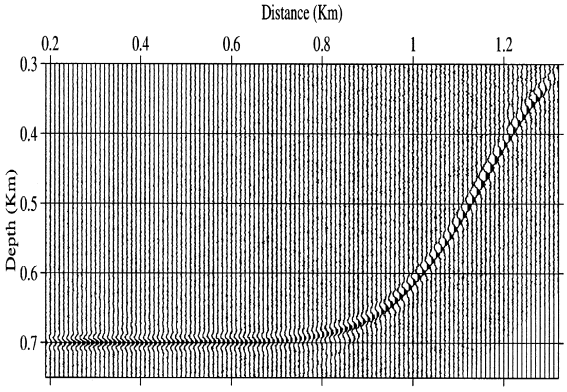

Fig. 3. 2.5-D true-amplitude depth migrated seismic data, real part, obtained after migrating the synthetic seismic data in Fig. 1.

(1985), which does not allow for any caustics along rays.

The above weight function is to be applied to the amplitude of the 2.5-D seismic data, that is generated when we have a situation of a point source lined up to a set of receivers in the plane $\xi_2 = 0$, by considering a seismic model where the velocity field does not depend on the second coordinate ξ_2. If the chosen point M inside the model coincides with a real reflection point R and $\xi = \xi^*$, the result of applying the difraction stack migration operator (Eq. (28)) to the seismic data is proportional to the reflection coefficient. Putting this result into the point R, we have the so-called true-amplitude depth migrated reflection data. In cases of special configurations, we can apply the weight function (34) as follows: (1) Common-offset: $\Gamma_G = \Gamma_S = 1$ for $S \neq G$; (2) Common-shot: $\Gamma_S = 0$ and $\Gamma_G = 1$ when the source point S is fixed; (3)

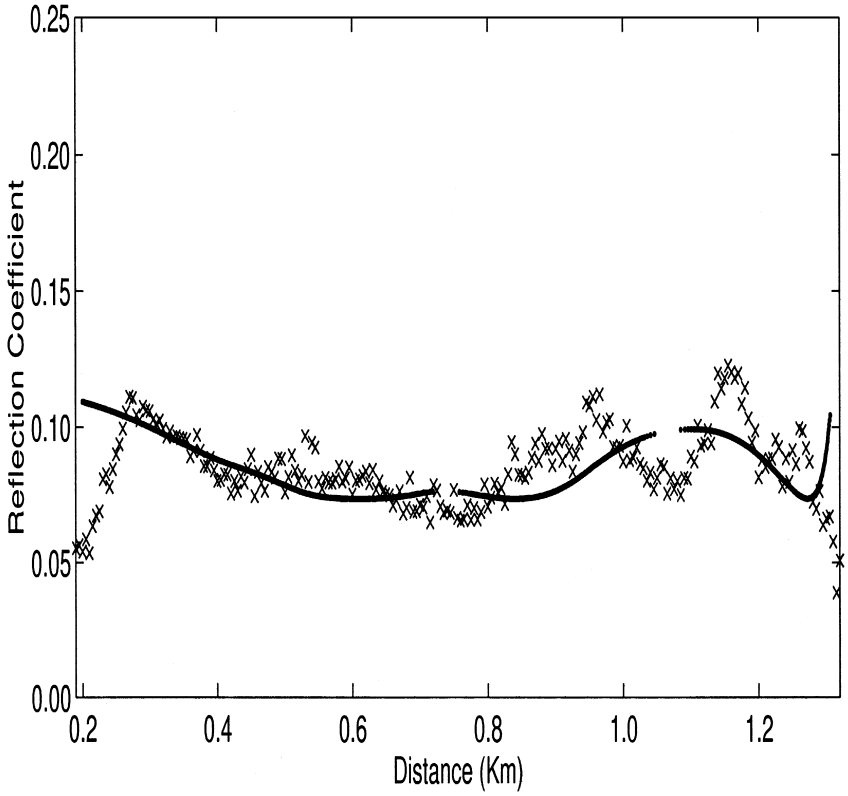

Fig. 4. In the cross line, we have the reflection coefficients picked from the reflector position in the migrated data. The continuous line corresponds to the exact value of the reflection coefficient. In the continuous line, the gaps correspond to the reflector region where there is no illumination. In the migrated result these gaps are filled by interpolated values from the migration operator.

Common-receiver: $\Gamma_S = 1$ and $\Gamma_G = 0$ when the receiver point G is fixed; and (4) Zero-offset: $\Gamma_S = \Gamma_G = 1$ for $S \equiv G$, and then $\alpha_S = \alpha_G$, $\kappa_1 = \kappa_2$ and $\sigma_S = \sigma_G$. In the common-midpoint configuration, the weight function is not adequate because in this case, the stationary phase solution is not valid.

4. Application of 2.5-D true-amplitude migration

The true-amplitude migration algorithm was tested on synthetic data obtained from the SEIS88 ray tracing software. The seismic model is constituted by a layer above an arbitrary curved reflector (Fig. 2). The interval velocity of the P–P wave in the overburden is 2.5 km/s, and 3.0 km/s in the half-space. The seismic data was generated into a common-shot configuration, with the source at $x = 0.1$ km in the earth surface and 177 geophones positioned between 0.3 and 1.4 km, being the geophone interval distance 6.25 m. The source pulse is represented by a Gabor wavelet as proposed by Gabor (1946), with frequency 80 Hz, while the seismic trace has the sample interval of 0.5 ms. In the seismic data a random noise with uniform distribution was added, in which the maximum value is 10% of the maximum amplitude of the seismic data. The macro-velocity model and the seismogram with noise are presented in Fig. 2. The seismic data were migrated by using the true constant velocity model, having the target zone $0.19 \le x \le 1.32$ km; $0.3 \le z \le 0.75$ km, with $\Delta x = 5$ m and $\Delta z = 1$ m. The migrated seismic image (real part) is presented in Fig. 3. In Fig. 4, we have the reflection coefficients, where the continuous line corresponds to the exact values, while the crosses indicate the amplitudes determined from the migrated section. As a consequence of the addition of noise to the input data, the seismic migration algorithm does not correctly recover the original source wavelet. But even in spite of the noise, we can see that the obtained seismic image represents the true reflector very well. In case of noise in the data, it is not so easy to determine where the so-called boundary effects begin to influence the migrated data.

5. Seismic inversion method

Based on the Born and on the ray theoretical approximations, Bleistein (1987) and Tygel et al. (1993), respectively, presented a new inversion method, the so-called DDS, through which it is possible to estimate several parameters on the trajectory of a selected ray between the source and geophone, for any arbitrary configuration of the seismic data. This inversion technique is based on the weighted diffraction stack migration integral, used above for determining the reflection coefficient. In this paper, the DDS inversion technique is used to determine three

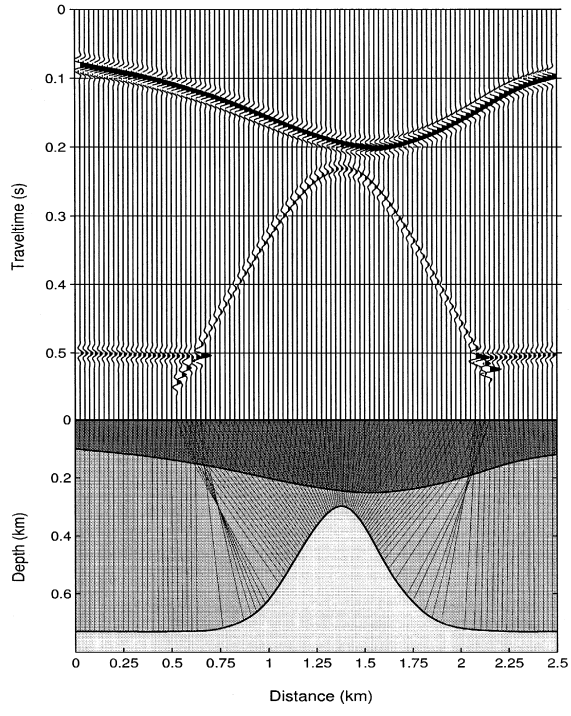

Fig. 5. Synthetic seismic data, used as input in the DDS inversion technique. The seismic model is constituted by two layers above a half-space, with velocities 2500 m/s (upper layer) and 3000 m/s (bottom layer).

parameters related to the trajectory of the normal reflection ray, to be known: (1) the radius of curvature, R_{NIP}, of the Normal Incidence Point (NIP) wave associated with the normal ray; (2) the emergence point x_o of the normal reflection ray; and (3) the emergence angle β_o of the normal reflection ray. The NIP wave, as defined by Hubral (1983), is a hypothetical wave that starts at the reflection point at time zero, propagates with half the medium velocity and returns to the earth surface at the two-way time of the normal ray.

By applying the DDS inversion technique, we make use of the weighted diffraction stack integral. Alternatively, we write $V(M,t) = V_j(M,t)$, where j is the index for specifying the

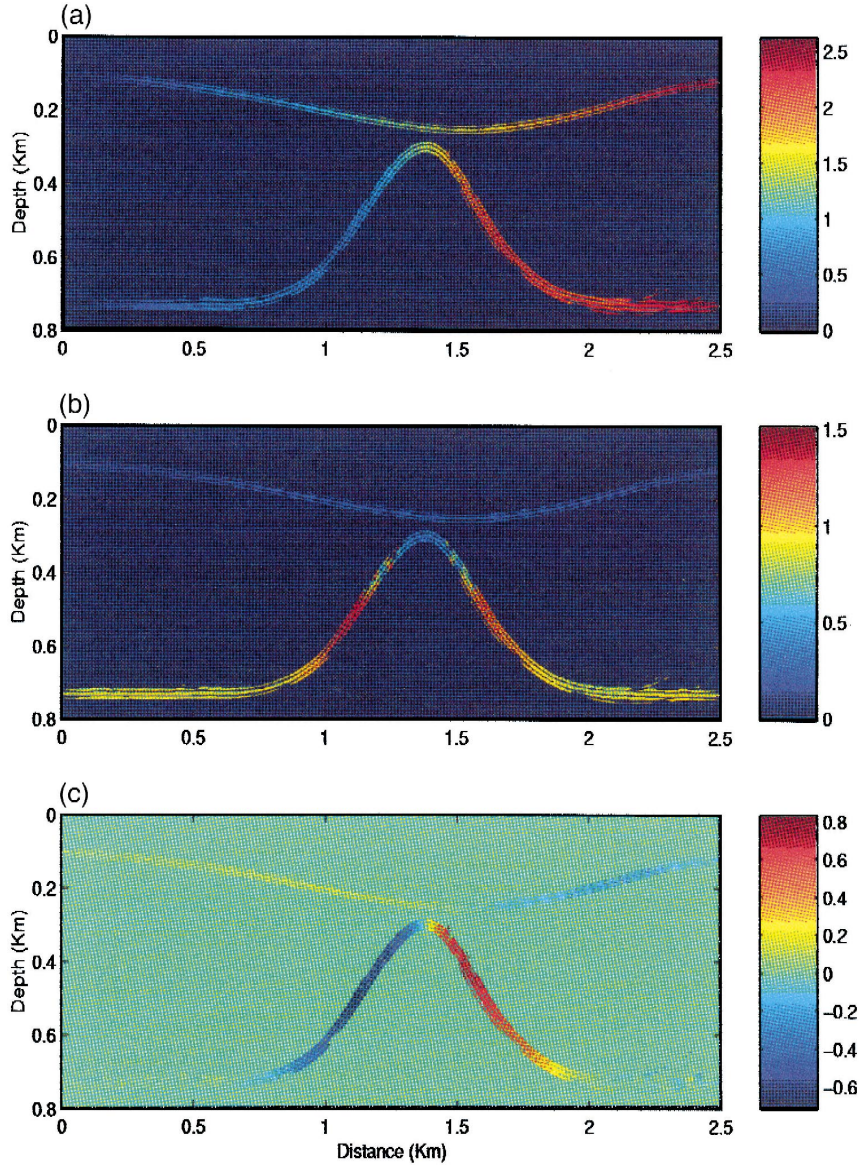

Fig. 6. Final products of the DDS inversion technique: (a) coordinate of the emergence points of the normal reflection rays; (b) radii of curvatures of the NIP waves; (c) emergence angles of the normal reflection rays.

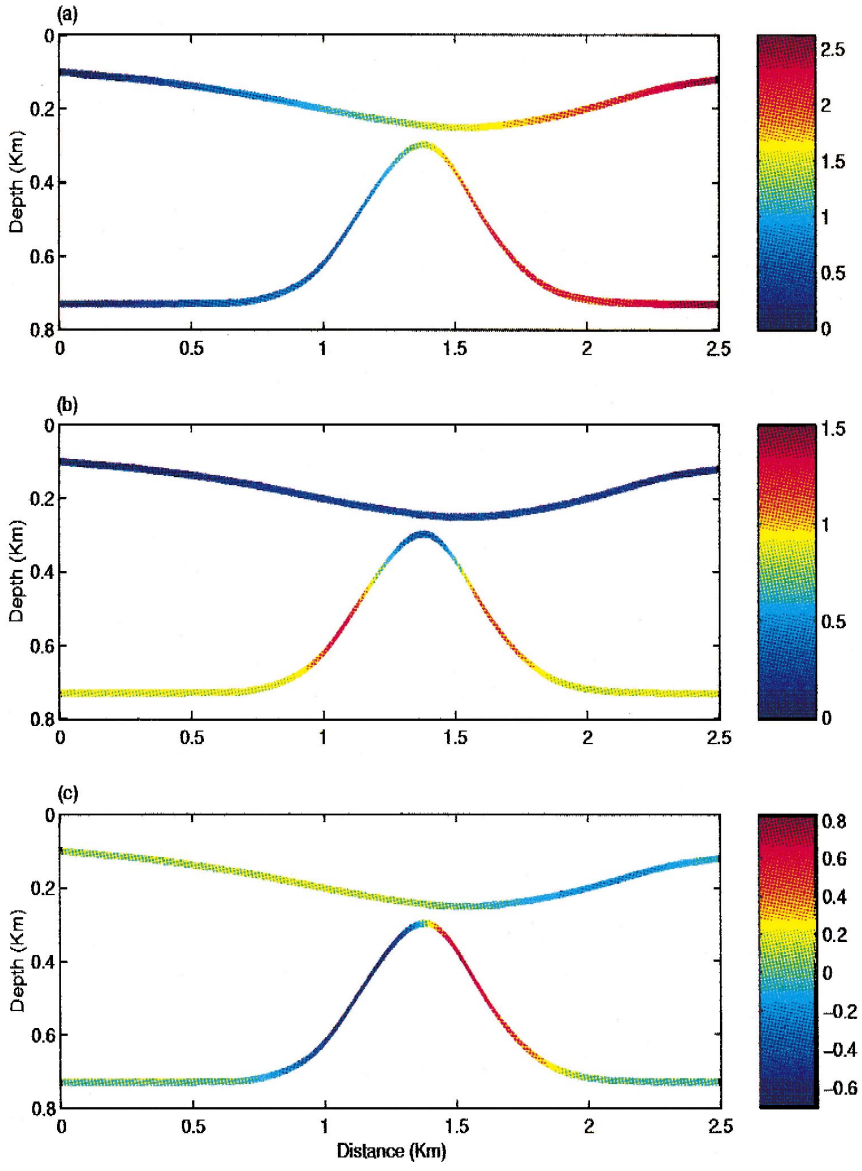

Fig. 7. Exact values of wavefront parameters calculated by ray theory: (a) coordinate of the emergence points of the normal reflection rays; (b) radii of curvatures of the NIP waves; (c) emergence angles of the normal reflection rays.

used weight to stack the input data. The DDS inversion technique is then done by a double stack, each one with a different weight function $j=1$ and $j=2$. The result is obtained by the ratio between the two stacks given by:

$$V_{\mathrm{DDS}}(M,t)=\frac{V_1(M,t)}{V_2(M,t)}. \tag{36}$$

If we choose as the weight function for the first stack a ray parameter specified by the trajectory starting at point M in the reflection point up to the earth surface, and for the second stack the unity, the V_{DDS} will result in the value of the selected ray parameter. In this paper, we have used for the first stack the values of R_{NIP}, x_{o} or β_{o}, calculated for each one of the diffraction trajectories starting at a point M within the

subsurface, having as input data a zero-offset seismic section. The result of this inversion technique is a mapping of normal ray parameters associated with primary reflection events in the zero-offset data. By choosing a minimum amplitude value in the denominator of the formula (36), we have empirically avoided the division by zero in the DDS algorithm.

6. Application of the DDS

In order to do a numerical experiment, we have generated a set of zero-offset seismic traces by using the ray theoretical modeling algorithm SEIS88. We have used the seismic model of Fig. 5 constituted by two layers above a half-space with two reflectors. The $P-P$ wave velocities are 2500 and 3000 m/s for the first (upper) and second (bottom) layers, respectively. By using a Gabor wavelet as proposed by Gabor (1946) with a frequency of 60 Hz, a sample interval of $\Delta t = 1$ ms and a space interval $\Delta x = 25$ m, we have obtained an ensemble of zero-offset seismograms (Fig. 5) used as input data in the DDS process. The final products are obtained by using the same P-wave velocities of the original seismic model, in order to find the following parameters of the normal rays at the second interface: (1) the coordinates of the emergence points of the reflection normal rays (Fig. 6a); (2) the radii of curvatures (radiusgram) of the NIP waves associated with each reflection normal ray (Fig. 6b); and (3) the emergence angles of the reflection normal rays (anglegram) (Fig. 6c). As we can see in Fig. 7a, b and c, the obtained values by DDS technique are very similar to the true values, which provides an evaluation of the accuracy of the proposed inversion method.

In the above results, we have shown that the DDS inversion technique can be used for determining a selected parameter along the ray trajectory. The three parameters here obtained (R_{NIP}, β_{o}, x_{o}) are the key for solving the interval velocity inversion problem. A more detailed discussion about the inverse problem can be found in Hubral and Krey (1980).

7. Conclusion

Starting from the paraxial ray theory, we have derived a 2.5-D weight function to be used in the 2.5-D diffraction stack migration operator. Based on the double diffraction stack inversion technique, we have also built an algorithm to determine fundamental parameters related to the normal ray trajectory. From the results obtained in this paper, we claim that the present 2.5-D weight function when applied to the 2.5-D seismic data is able to recover the reflection coefficient even in a noisy environment. The 2.5-D true-amplitude migration algorithm is stable, i.e., we have that small perturbation in the input data provides only slight deviation in the output migrated data. It is to be stressed that the proposed 2.5-D true-amplitude migration algorithm works very good in more complex situations when there are triplications in the input data due the presence of caustics. In addition, we have shown that the DDS inversion technique is able to determine parameters along the ray trajectory that are of interest for the interval velocity inversion problem.

Acknowledgements

We thank the $\mathrm{CNP_q}$ for supporting one of the authors of this research, Prof. Dr. M. Tygel of the IMEC/UNICAMP/Brazil for the fruitful discussions during the preparation of this paper, and the seismic work group of the Charles University, Prague, Czech Republic, for making the ray tracing software SEIS88 available to us. We also thank for the important suggestions of three anonymous reviewers of the Karlsruhe University Workshop on Macro Velocity Indendent Seismic Imaging.

Appendix A

Following Schleicher et al. (1993), the weighted modified diffraction stack is considered an appropriate method to perform a true-amplitude migration. For each point M in the macro-velocity model and all points (ξ_1,ξ_2) in the migration aperture A, the diffraction stacks are then performed by summation along the Huygens surfaces $\tau_D(\xi_1,\xi_2,M)$ for all points M into a region of the model. The true-amplitude migration is achieved by the summation using certainly Huygens surface and derived weight function, such that the stack output is proportional to the desired reflection coefficient. Mathematically, this operation is described by the 2-D integral

$$V(M,t)=\frac{-1}{2\pi}\int\int_A \mathrm{d}\xi_1\mathrm{d}\xi_2 w(\boldsymbol{\xi},M)\dot{U} \times(\boldsymbol{\xi},t+\tau_D(\boldsymbol{\xi},M)), \quad \text{(A1)}$$

where the symbol $(\cdot)$ means the first derivative with respect to time, and $w(\boldsymbol{\xi},M)$ is the weight function used to stack.

By transforming the expression (A1) into the frequency domain:

$$\hat{V}(M,\omega)=\frac{-i\omega}{2\pi}\int\int_A \mathrm{d}\xi_1\mathrm{d}\xi_2 w(\boldsymbol{\xi},M)\hat{U}(\boldsymbol{\xi}) \times\exp[i\omega\tau_D(\boldsymbol{\xi},M)]. \quad \text{(A2)}$$

In order to specialize the 3-D formula (A2) to the 2.5-D geometry, we start considering $M=R$, i.e., the reflection point itself. The migration integral needs to be solved asymptotically by the stationary phase method as found in Bleistein (1984) with respect to the coordinate ξ_2, by making use of the stationary condition as showed in Bleistein et al. (1987):

$$\frac{\partial\tau_D}{\partial\xi_2}=\frac{\partial\tau(S(\boldsymbol{\xi}),R)}{\partial\xi_2}+\frac{\partial\tau(R,G(\boldsymbol{\xi}))}{\partial\xi_2}\Big|_{\Sigma_o}=0, \quad \text{(A3)}$$

which can be expressed through the identity:

$$\frac{\partial}{\partial\xi_2}[\tau(S,M)+\tau(M,G)]|_{\Sigma_o}=p_{2s}+p_{2g}|_{\Sigma_o}=0. \quad \text{(A4)}$$

By applying the in-plane ray condition $p_2=p_{2o}$ into the 3-D ray equation as given by Cervený (1987), we have:

$$x_{2s}=\sigma_s p_{2s}|_{\Sigma_o} \text{ and } x_{2g}=\sigma_g p_{2g}|_{\Sigma_o}, \quad \text{(A5)}$$

with σ_s and σ_g calculated along the ray paths SM and MG, respectively. By considering the 2.5-D geometry, $x_{2s}=x_{2g}=\xi_2$, we finally have the result:

$$p_{2s}+p_{2g}\Big|_{\Sigma_o}=\left(\frac{1}{\sigma_s}+\frac{1}{\sigma_g}\right)\Big|_{\Sigma_o}\xi_2=0. \quad \text{(A6)}$$

From Eq. (A6), we conclude that the stationary phase condition is $\xi_2=0$. For completeness of our asymptotic analysis, we calculate the second derivative of the phase at $\xi_2=0$

$$\frac{\partial^2}{\partial\xi_2^2}[\tau(S,R)+\tau(R,G)]\,|_{\xi_2=0}=\frac{1}{\sigma_S^o}+\frac{1}{\sigma_G^o}. \quad \text{(A7)}$$

Here, σ_S^o and σ_G^o are the ray parameters for the ray branches RS and RG, calculated on the earth surface Σ_o.

The above results yield the stationary phase solution

$$\hat{V}(R,\omega)\approx\frac{\sqrt{-i\omega}}{\sqrt{2\pi}}\int_A \mathrm{d}\xi\, w(\xi,R) \times\left(\frac{1}{\sigma_S^o}+\frac{1}{\sigma_G^o}\right)^{-1/2}\hat{U}(\xi,\omega) \times\exp[i\omega\tau_D(\xi,R)], \quad \text{(A8)}$$

As a consequence of the fact that $\hat{U}(\xi,\omega)$ is the in-plane observed point-source wavefield amplitude factor, the 2.5-D weight function is defined as:

$$w_{2.5}(\xi,R)=w(\xi,R)\left(\frac{1}{\sigma_S^o}+\frac{1}{\sigma_G^o}\right)^{-1/2}, \quad \text{(A9)}$$

where $w(\xi, R)$ is the in-plane version of the 3-D weight function of the 3-D modified diffraction stack by Schleicher et al. (1993). The weight expression (A9) can be readily generalized to any arbitrary depth point M.

References

Beylkin, G., 1985. Imaging of discontinuities in the inverse scattering problem by inversion of a causal generalized radon transform. J. Math. Phys. 26, 99–108.

Bleistein, N., 1984. Mathematics of Wave Phenomena. Academic Press.

Bleistein, N., 1986. Two-and-one-half dimensional in-plane wave propagation. Geophys. Prospect. 34, 686–703.

Bleistein, N., 1987. On the imaging of reflectors in the earth. Geophysics 52, 931–942.

Bleistein, N., Cohen, J.K., Hagin, F.G., 1987. Two and one-half dimensional Born inversion with an arbitrary reference. Geophysics 52, 26–36.

Bortfeld, R., 1989. Geometrical ray theory: rays and traveltimes in seismic systems (second-order approximation of the traveltimes). Geophysics 54, 342–349.

Cervený, V., 1987. Ray Methods for Three-dimensional Seismic Modeling. Norwegian Institute for Technology.

Gabor, D., 1946. Theory of communication. J. IEEE 93, 429–441.

Hanitzsch, C., 1997. Comparison of weights in prestack amplitude-preserveing Kirchhoff depth migration. Geophysics 62, 1812–1816.

Hubral, P., 1983. Computing true amplitude reflections in laterally inhomogeneous earth. Geophysics 48, 1051–1062.

Hubral, P., Krey, T., 1980. Interval Velocities from Seismic Reflection Time Measurements. SEG.

Hubral, P., Tygel, M., Zien, H., 1991. Three-dimensional true-amplitude zero-offset migration. Geophysics 56, 18–26.

Liner, C., 1991. Theory of a 2.5-D acoustic wave equation for constant density media. Geophysics 56, 2114–2117.

Martins, J.L., Schleicher, J., Tygel, M., Santos, L.T., 1997. 2.5-D true-amplitude migration and demigration. J. Seism. Explor. 6, 159–180.

Schleicher, J., Tygel, M., Hubral, P., 1993. 3-D true-amplitude finite-offset migration. Geophysics 58, 1112–1126.

Stockwell, J.W., 1995. 2.5-D wave equations and high-frequency asymptotics. Geophysics 60, 556–562.

Tygel, M., Schleicher, J., Hubral, P., Hanitzsch, C., 1993. Multiple weights in diffraction stack migration. Geophysics 57, 1054–1063.

Tygel, M., Schleicher, J., Hubral, P., 1996. A unified approach to 3-D seismic reflection imaging: Part 2. Theory. Geophysics 61 (3), 759–775.

Ursin, B., 1982. Quadratic wavefront and traveltime approximations in inhomogeneous layered media with curved interfaces. Geophysics 47, 1012–1021.